Computers and Concrete, *Vol. 18, No. 3 (2016) 389-404*
DOI: http://dx.doi.org/10.12989/cac.2016.18.3.389

Behavior of reinforced concrete plates under impact loading: different support conditions and sizes

Metin Husem* and Suleyman I. Cosgun[a]

Department of Civil Engineering, Karadeniz Technical University, Trabzon, Turkey

(Received October 30, 2014, Revised February 19, 2016, Accepted April 20, 2016)

Abstract. In this study, effects of impact loads on reinforced concrete (RC) plates are examined analytically. During examination of RC plates, they were exposed to impact loading with two different support conditions in three different sizes. RC plates in different support conditions were analyzed with Concrete Damage Plasticity Model (CDP) and reinforcing steel was modeled with Classical Metal Plasticity Model (CMP) by ABAQUS finite element software. After the analysis it is found that impact loads, displacements, energy absorption capacities and damage patterns are changed due to support conditions and plate sizes. Results that are obtained from RC plate experiments in literature under impact loads are found to be similar with the results of numerical analysis with CDP material models.

Keywords: impact load; RC plates; CDP; CMP, energy absorption capacity; support conditions

1. Introduction

Concrete is a composite structural material that is widely used in common for both concrete and RC structures. Reinforced structures that are constructed with such materials are exposed to static (its own weight and live loads) and dynamic loads (earthquake, wind, etc.) during service periods. In addition to these loads, these structures can be exposed to impact and explosion effects nowadays. Generally nuclear plants, airports and military installations are exposed to explosion and impact loads. However, in normal structures, these conditions can be seen due to gas explosion and terrorist attacks. Because of this reason, in RC structures, the effect of impact loads that is gaining popularity should be investigated. Especially in recent years there are many studies related with the RC elements that are produced by concrete which has not sufficient strength under such effects both experimentally and theoretically. Some of these studies are conducted by Sawamoto *et al*. (1998), there is an analytical model was developed to determine local strains that can be possibly seen for RC panel elements. RC panels under the impact load which are caused by bullet impact were modeled by applying the discrete element method. Analysis results that are obtained from Discrete Element Method were compared with the results that were obtained from experimental studies. Abbas et.al (2004) were made numerically and experimentally studies for

*Corresponding author, Professor., E-mail: mhusem@ktu.edu.tr
[a]Ph.D., Student., E-mail: sicosgun@ktu.edu.tr

http://www.techno-press.org/?journal=cac&subpage=8 ISSN: 1598-8198 (Print), 1598-818X (Online)

defining the non-linear behaviors of RC plates and beams. The study that was conducted by Zineddin and Krauthammer (2007) has aims to examine behaviors of RC flooring under impact loads and increasing their element's impact strengths. These researchers searched for effects of impact strengths of RC floorings under different types of reinforcement arrangements. Chen and May (2009) conducted a research about the effects of objects by creating impact loads with higher weights and impact in low velocities on RC elements like beams, plates, etc. Martin (2010) searched with numerical modeling for structural behaviors of structural elements under impact load. Finite element models are searched for different structural behaviors under different material models. Effects of soft and hard impact loads were modeled both by deformable and rigid bullets. Studies that are conducted by Trivedi and Singh (2013) consist of numerical models to foresee the structural behaviors of RC under local strains that are exposed to impact loads. Similarities of the failure type and the fracture energy (Gf) values were obtained from between the experimental works and FEM analyses were conducted by Zineddin and Krauthammer (2007). Furthermore, some studies were performed to improve the impact behavior of concrete on basis of material. Perumal (2014) investigated high-performance steel fiber reinforced concrete under impact loading. According to experimental results, the additional of steel fibers to silica fume concrete improve impact behavior of high-performance concrete. Together with these studies it was aimed to search for numerical models with parameters like solution mesh size, strain rate, behavior of the reinforcing steel.

Many of other previous studies had intended to research the behaviors of the parameters such as, the velocity of impact object, the thickness of RC element, the compressive and tensile strength of concrete and reinforcement arrangement. In this study, different from the technical literature, RC plates with different span sizes are examined numerically for both free and fixed support conditions.

2. Properties of RC plates

The scope of this study is to conduct analysis for RC plates in three sizes under impact loads. Plates are accepted as fitting on free and fully bounded on support (fixed). Concrete Damage Model (CDP) is used for every support plates. For this reason, there are two analysis done for every plate due to impact loads by totally on six RC plates. Plates that are exposed to impact loads are shown in Table 1 with their properties. Impact load analysis of the plates is applied in same reinforcement arrangement. Because of that reason, one of the reinforcement arrangement and geometrical properties of plate PK1020 are given Fig. 1.

Table 1 RC plates that are used for impact loading

Plate Name	Sizes (mm)	Reinforcement Arrangement (sub-top)	Support Conditions
PK1011-1	1100×1100×100	Ø8/100- Ø8/100	Free
PK 1011-2			Fixed
PK 1020-1	2000×2000×100	Ø8/100- Ø8/100	Free
PK 1020-2			Fixed
PK 1030-1	3000×3000×100	Ø8/100- Ø8/100	Free
PK 1030-2			Fixed

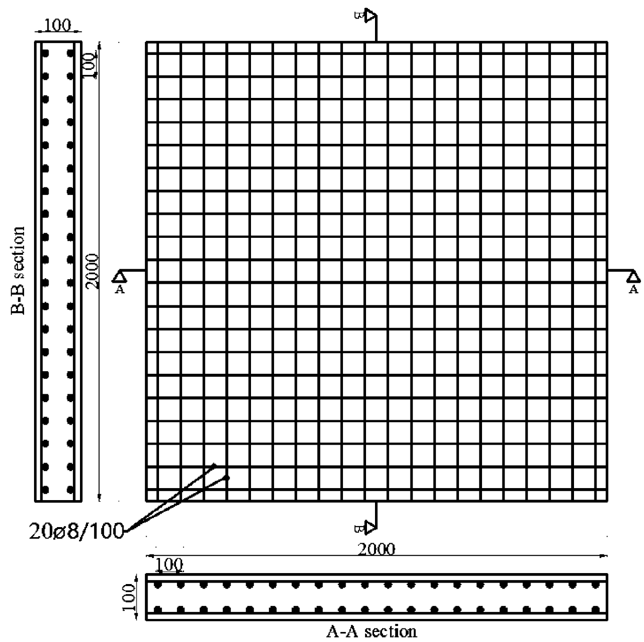

Fig. 1 Reinforcement plan for typical RC plate (PK1020)

3. Finite Element Model (FEM) of RC plates

FEM of the RC plates are created by ABAQUS software. Their sizes and reinforcement arrangement are given Table 1. RC plates were created with two separate elements. Concrete plates and reinforcing steel were modeled with C3D8R solid element and T3D2 truss element, respectively (see Fig. 2). In this study, C3D8R element that is used in more accurate finite element model dominated by inelastic behavior. In FEM analyses, C3D8R finite element was preferred. Because, this element shows accurate results in nonlinear behavior of structure systems. Concrete plate model that was created by using the combination of C3D8R and T3D2 elements are shown in Fig. 3.

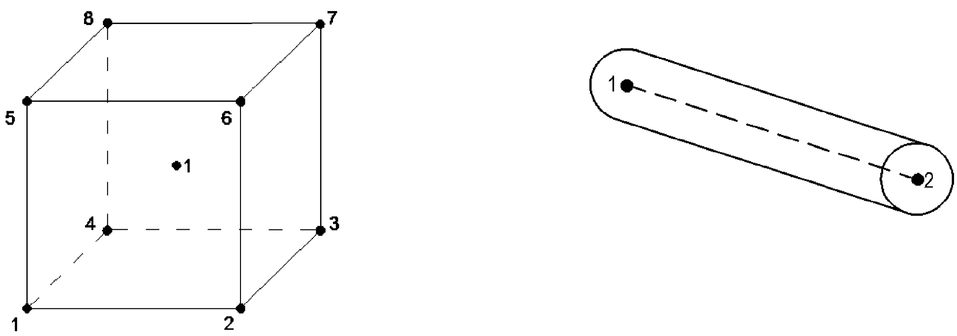

(a) C3D8R element (b) T3D2 element

Fig. 2 Finite elements used in modeling of RC plate

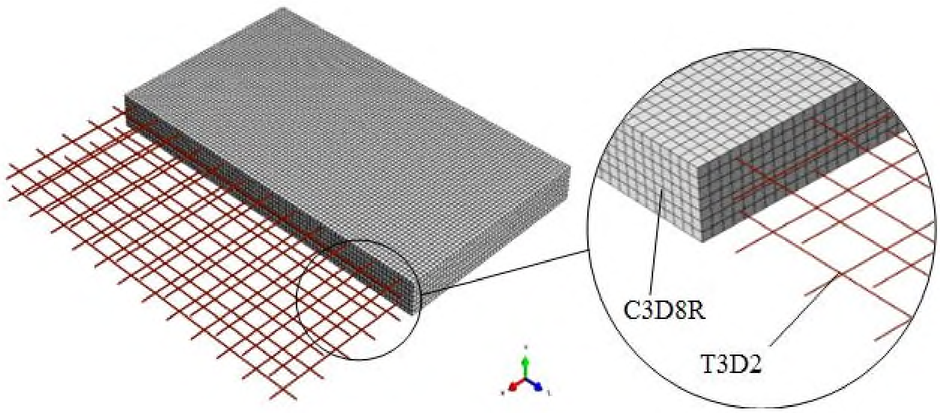

Fig. 3 FEM of the RC plates

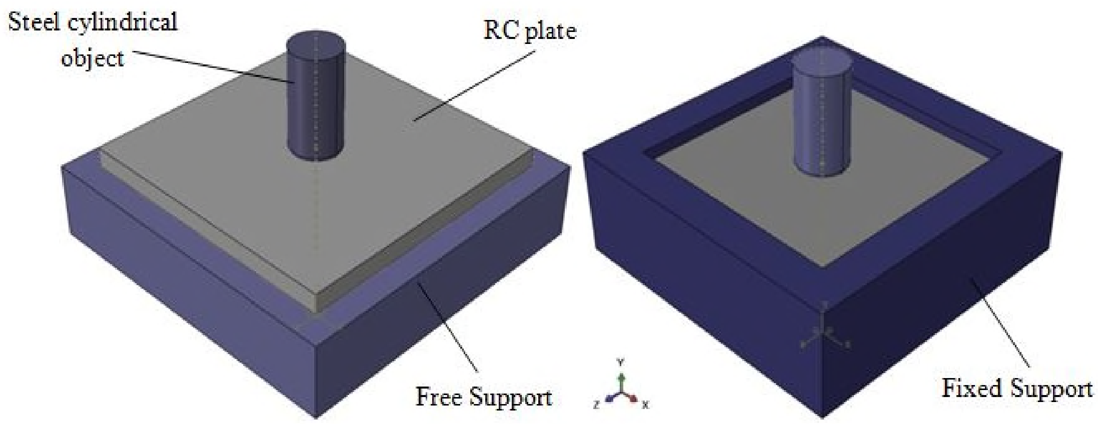

Fig. 4 Support conditions of RC plates

In this study, finite element models were created for RC plates these are fixed and free supports. Stresses and strains which are occurred in supports are not in scope of this study so that size of the finite element mesh sizes were chosen bigger than compared to RC plate models. By this way finite element models of the support plates are shown in Fig. 4. Steel cylindrical object (diameter 200mm, height 410mm) which are used to create impact loading on RC plates was impacted to plates with different support conditions to represent mass with m=100kg and free fall from h=3m with V_d=7.67m/s velocity. V_d was determined as, the speed value that occurred just before the impact of a mass which dropped from a certain height, to RC plate. Here, by conservation of the energy, the speed on impact (V_d) was calculated by the Eqs. (1-2).

$$mgh = \frac{1}{2}mV_d{}^2 - \frac{1}{2}mV_i \qquad \text{Initial velocity of mass } (V_i=0) \tag{1}$$

$$V_d = \sqrt{2gh} = \sqrt{2.9{,}81.3{,}00} = 7{,}67\ m/s \tag{2}$$

4. Constitutive model of concrete

4.1 Concrete Damage Plasticity (CDP) Model

RC plates that were used for finite element models have strength class of the concrete C30 (compressive strength of concrete is 30 MPa). It must be known about the concrete that defined to use modeling of RC plates which are exposed to impact load, the changes of compressive and tensile strength due to strain rate. The increase coefficient was taken 1.30 corresponding to the strain rate 1.0 1/s from scale of Ammann and Nussbaumer (1995). Stress-strain relation curves that under effects of uniaxial compression and tensile of the concrete, were used to modeling of RC plates, are given Fig. 5.

CDP model is used for ABAQUS software to model plain or RC members. This model was proposed by Lubliner *et.al* (1989), for static loadings and after that it was improved by Lee and Fenves (1998) for dynamic and cycling loading conditions. In addition, the stiffness degradation of material has been considered in CDP model under compression and tension behaviors. Lee and

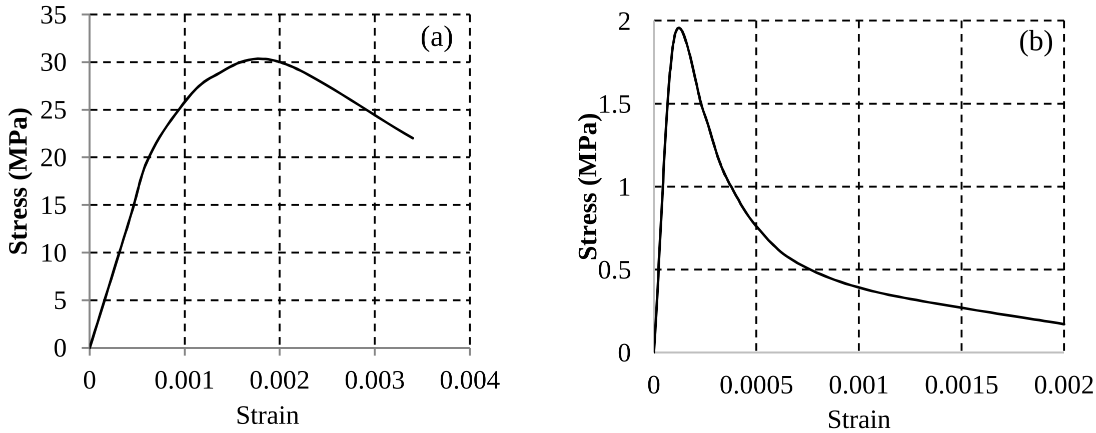

Fig. 5 Stress-strain curves of concrete under uniaxial compressive (a) and tensile (b)

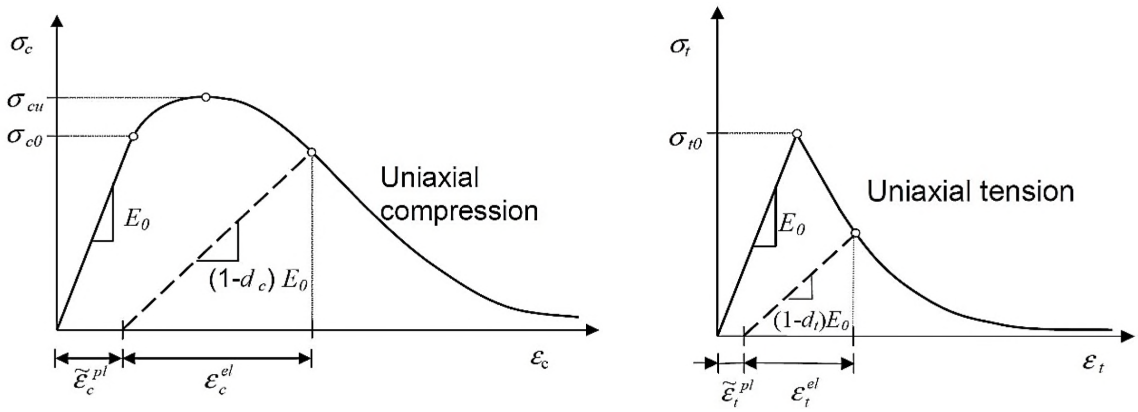

Fig. 6 CDP model with the stress-strain relations of concrete under uniaxial compression and tension (ABAQUS, 2008)

Fenves (1998) was defined two different scalar variables (d_c, d_t). In accordance to this change in elastic modulus of the concrete is defined as

$$E = (1 - d_{t,c})E_0 \tag{3}$$

In here, d_t and d_c are parameters of degradation in stiffness in compression and tension and E_o is the initial elastic modulus. As it can be understood from Eq. (3) two damage parameters are changing between 0<d<1 interval. When it is equal to d=0, this situation shows that the material is undamaged. In another condition, d=1, stiffness degradation cannot be controlled. Both of these conditions, it is not possible to define behavior of the concrete (Fig. 6). In these variables d_c is controlling the stiffness degradation under uniaxial compression and d_t is controlling the stiffness degradation under uniaxial tension.

Behavior of the concrete under the uniaxial loading in CDP model, ε_c^{in} for uniaxial compression and ε_t^{ck} for uniaxial tension for strain values are defined Eqs. (4)-(5). These strains are respectively as inelastic and cracking strains. They were calculated by following equations according to Hibbit *et al.* (2011). In the ABAQUS software, the uniaxial stress-strain relations of concrete are converted into stress-plastic strain relations with damage parameters $(d_{t,c})$ and inelastic and cracking strains automatically. These strains are given in Eqs. (6)-(7).

$$\varepsilon_c^{in} = \varepsilon_c - \frac{\sigma_c}{E_0} \tag{4}$$

$$\varepsilon_t^{ck} = \varepsilon_t - \frac{\sigma_t}{E_0} \tag{5}$$

$$\varepsilon_c^{pl} = \varepsilon_c^{in} - \frac{d_c}{1 - d_c} \cdot \frac{\sigma_c}{E_0} \tag{6}$$

$$\varepsilon_t^{pl} = \varepsilon_t^{ck} - \frac{d_t}{1 - d_t} \cdot \frac{\sigma_t}{E_0} \tag{7}$$

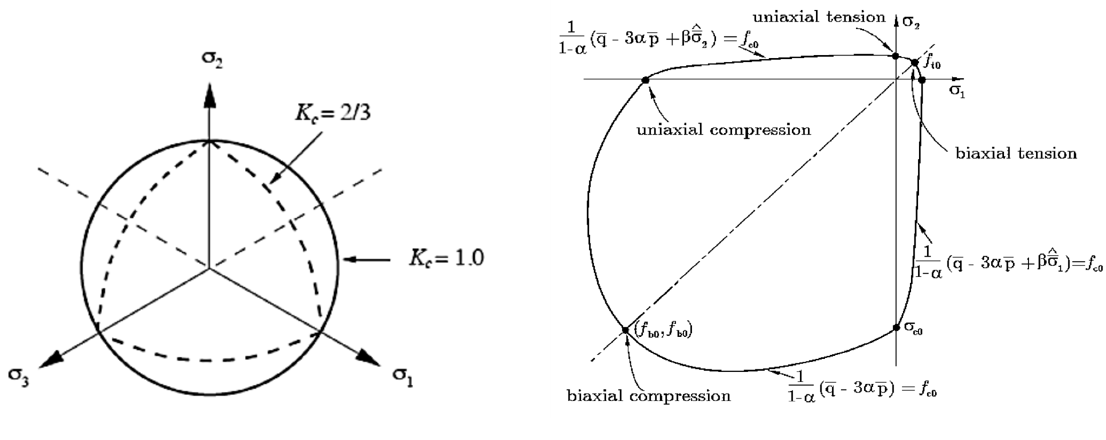

(a) (b)

Fig. 7 Yield surfaces in (a) deviatoric plane and (b) plane stress (ABAQUS 2008)

4.2 Plasticity of concrete

In CDP model, yield surface function is defined for concrete plasticity (Eq. (8)). This yield function was developed by Lubliner *et.al* (1989), with the modifications which were proposed by Lee and Fenves (1998). The evolution of the yield surface is controlled by the hardening variables ($\varepsilon_c^{pla}, \varepsilon_t^{pla}$). In terms of effective stress, the yield function takes the form,

$$F \quad = \frac{1}{1-a}\left(\bar{q} - 3\alpha\bar{p} + \beta\left(\varepsilon_c^{pl}\right).\langle\bar{\sigma}_{max}\rangle - \gamma.\langle-\bar{\sigma}_{max}\rangle\right) - \bar{\sigma}_c\left(\varepsilon_c^{pl}\right) = 0 \tag{8}$$

In this function, and are representing Mises equivalent stress and hydrostatic pressure respectively. Strains (ε_c^{pla}), (ε_t^{pla}) as it can be seen in Eqs. (4)-(5), $\bar{\sigma}_{max}$ is the maximum principal effective stress; ($\frac{f_{bo}}{f_{co}}$) is ratio of initial equibiaxial compressive yield stress to initial uniaxial compressive yield stress. K_c is the parameter that determines the yield surface in deviator plane. Yield surface in deviator plane and plane stress is given in Fig.7. In ABAQUS, K_c was proposed to be taken as 0,667.

$$\alpha = \left[\left(\frac{f_{bo}}{f_{co}}\right) - 1\right] \Big/ \left[2\left(\frac{f_{bo}}{f_{co}}\right) - 1\right] \tag{9}$$

$$\beta = \frac{\bar{\sigma}_c\left(\varepsilon_c^{pl}\right)}{\bar{\sigma}_t\left(\varepsilon_t^{pl}\right)}(1-\alpha) - (1+\alpha) \tag{10}$$

$$\gamma = 3(1-K_c)/2K_c - 1 \tag{11}$$

where α, β and γ are dimensionless constants. These constants are calculated by automatically with K_c, (ε_c^{pla}), (ε_t^{pla}), ($\frac{f_{bo}}{f_{co}}$).

The CDP model assumes non-associated plastic flow rule (ABAQUS 2008). The Drucker-Prager hyperbolic plastic potential function (G) used in CDP in ABAQUS is illustrated in Eq. (12).

$$G(\sigma) = \sqrt{(e.\sigma_{to}.tan\Psi)^2 + \bar{q}^2} - \bar{p}.tan\Psi \tag{12}$$

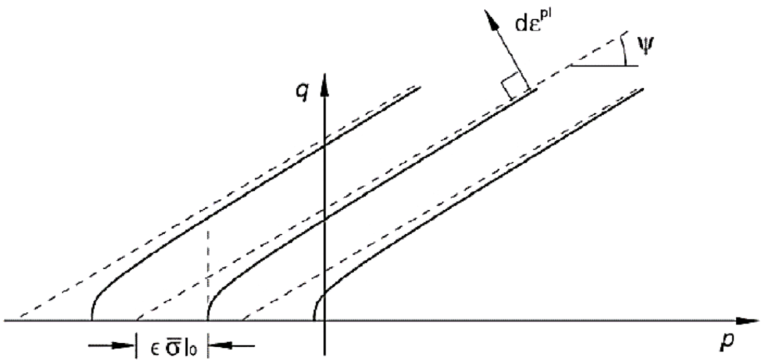

Fig. 8 Obtaining dilatation angle (Hibbitt 2011)

Table 2 Material properties and parameters of the concrete

Initial modulus of elasticity, E_o (MPa)	32000
Poisson ratio, ν	0.2
Density, ρ (kg/m^3)	2400
Compressive strength, f_{ck} (MPa)	30
Peak strain of compressive, ε	0.002
Ultimate strain, ε_u	0.0034
Tensile strength, f_{ctk} (MPa)	1.9
Dilation angle, Ψ	36
Eccentricity, e (ABAQUS, 2008)	0.01
Max. damage parameter of tensile, dt	0.99
Ratio of the second stress invariant on the tensile meridian to that on the compressive meridian, K_c (ABAQUS, 2008)	0.667
Ratio of initial equibiaxial compressive yield stress to initial uniaxial compressive yield stress, f_{bo}/ f_{co}(ABAQUS, 2008)	1.16

where σ_{to} is the uniaxial tensile stress at failure taken from user defined tension stiffening data. Ψ is the dilation angle measured in the $\bar{p}$- $\bar{q}$ plane at high confining pressure (see Fig. 8). This parameter controls the amount of plastic volumetric strain developed during plastic yielding (Kamali, 2012). Typically, the dilation angle value is taken between 35 and 40 (Malm, 2009). Other parameter (e) at Eq. (12) is defined as eccentricity in plastic potential function at asymptotes. Parameters that are used to define constitutive model of concrete are given in Table 2.

5. Material model of reinforcing steel

Classical Metal Plasticity (CMP) is a material model for behavior under uniaxial tensile loading of reinforcing steel. In this model elastic and plastic behavior of the material is thought to be separated. The elastic behavior is defined with elastic modulus (E) and poisson ratio (ν). Plastic behavior of reinforcing steel is defined true stress (σ_{tru}) and plastic strain (ε_{pl}). The nominal strain-stress curve can be converted to plastic strain-true stress curve according to Eqs. (13)-(15). see Hibbitt *et al*. (2011). In this model, yield strength of reinforcing steel is 420 MPa that the nominal strain-stress curve is given at Fig. 9.

$$\sigma_{tru} = \sigma_{nom}(1 + \varepsilon_{nom}) \tag{13}$$

$$\varepsilon_{tru} = \ln(1 + \varepsilon_{nom}) \tag{14}$$

$$\varepsilon_{pl} = \varepsilon_{tru} - \frac{\sigma_{tru}}{E} \tag{15}$$

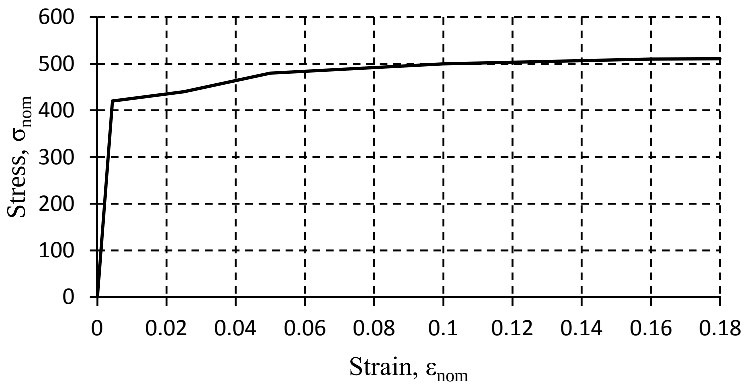

Fig. 9 Nominal stress-strain curve of the reinforcing steel

6. Results and discussion

Within the scope of this study, two different support and six RC plates in three different dimensions in 100 kg of mass and 7.67 m/sec velocity were used. In this study, transient impact load and mid span deflection of RC plates were obtained. Changes in PK1011, PK1020 and PK1030 plates with impact load and displacements are given in Fig. 10, Fig. 11 and Fig. 12 respectively. All impact analysis of the plates within the scope of this study are given in Table 3 for impact value and displacement values.

As it can be seen in these figures and Table 3, maximum of the impact load of PK1011-2 plate is %15 higher than the maximum impact load of PK1011-1, maximum impact load gained from PK1020-2 plate is %17 higher than the maximum impact load of PK1020-1, and maximum impact load handled from PK1030-2 is %24.5 higher than PK1030-1. When the mid-span of the plates is considered, maximum displacements were changed in important levels in accordance with the support conditions. When plates are in free support, mid-span displacement of the plate is decreased after maximum displacement value and fixed in certain value, in case of supports are

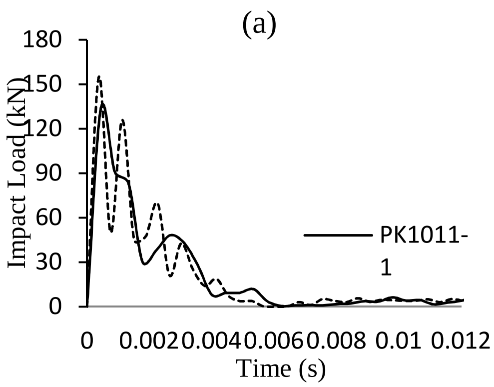

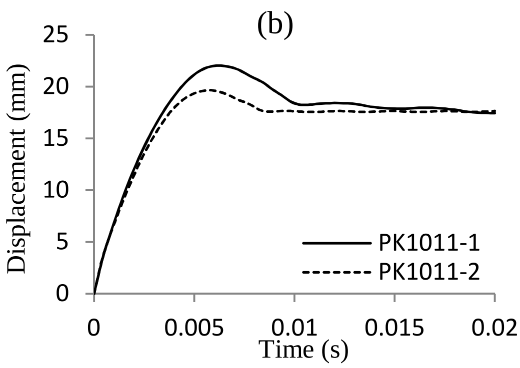

Fig. 10 PK 1011 series plates impact load-time (a), displacement-time curves (b)

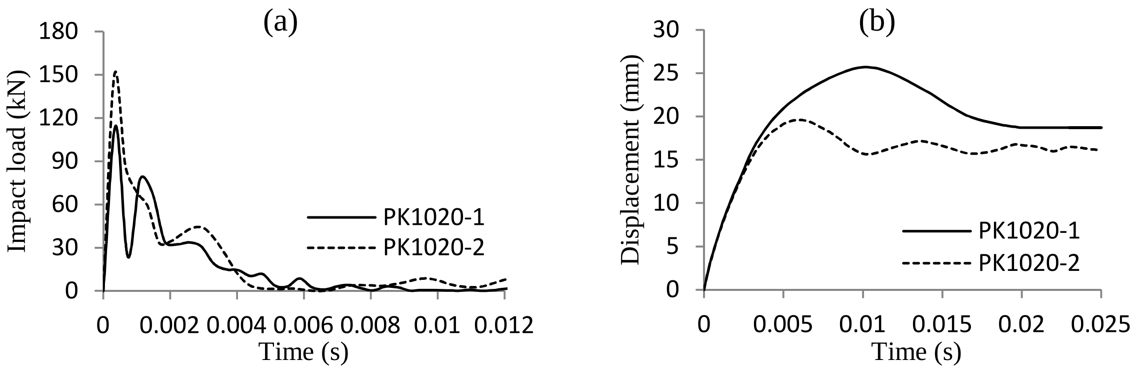

Fig. 11 PK 1020 series plates impact load-time (a), displacement-time curves (b)

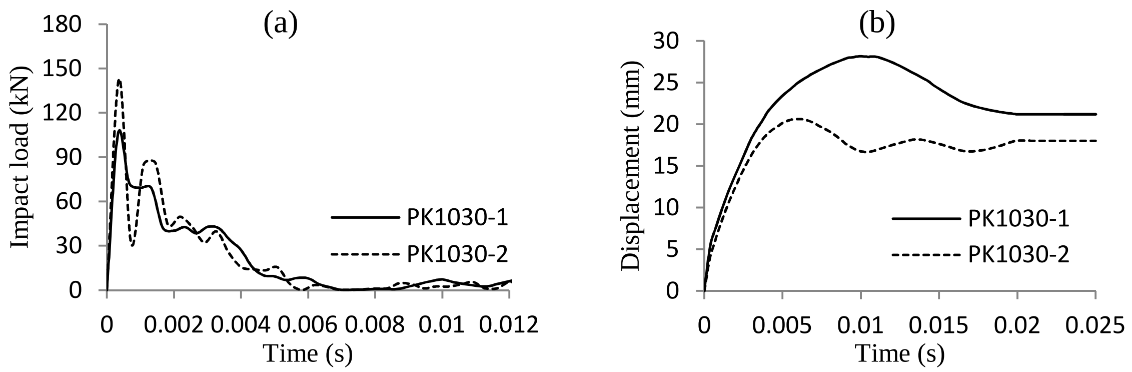

Fig. 12 PK 1030 series plates impact load-time (a), displacement-time curves (b)

Table 3 Results summary

Plates Name	Size (mm)	Impact Load (kN)	Maximum Displacement (mm)	Absorbed Energy (Joule)
PK1011-1	1000x1000x100	133.7	22	1204.4
PK1011-2		154.8	19.6	1172.7
PK1020-1	2000x2000x100	114.5	26	914.5
PK1020-2		150	20	1072.6
PK1030-1	3000x3000x100	105.8	28	836
PK1030-2		142.9	20.58	1041

fixed, maximum displacements are fixed in certain values similar with free support plates. Also as it can be observed from the figures, maximum mid-span displacements of free supported plates are increasing in parallel with values due to increase in plate span. Maximum displacement of PK 1030-1 is %8 higher than PK 1020-1 and %18 higher than PK 1011-1. Despite this, in fixed support conditions, increasing of plate span have no effect on maximum displacements.

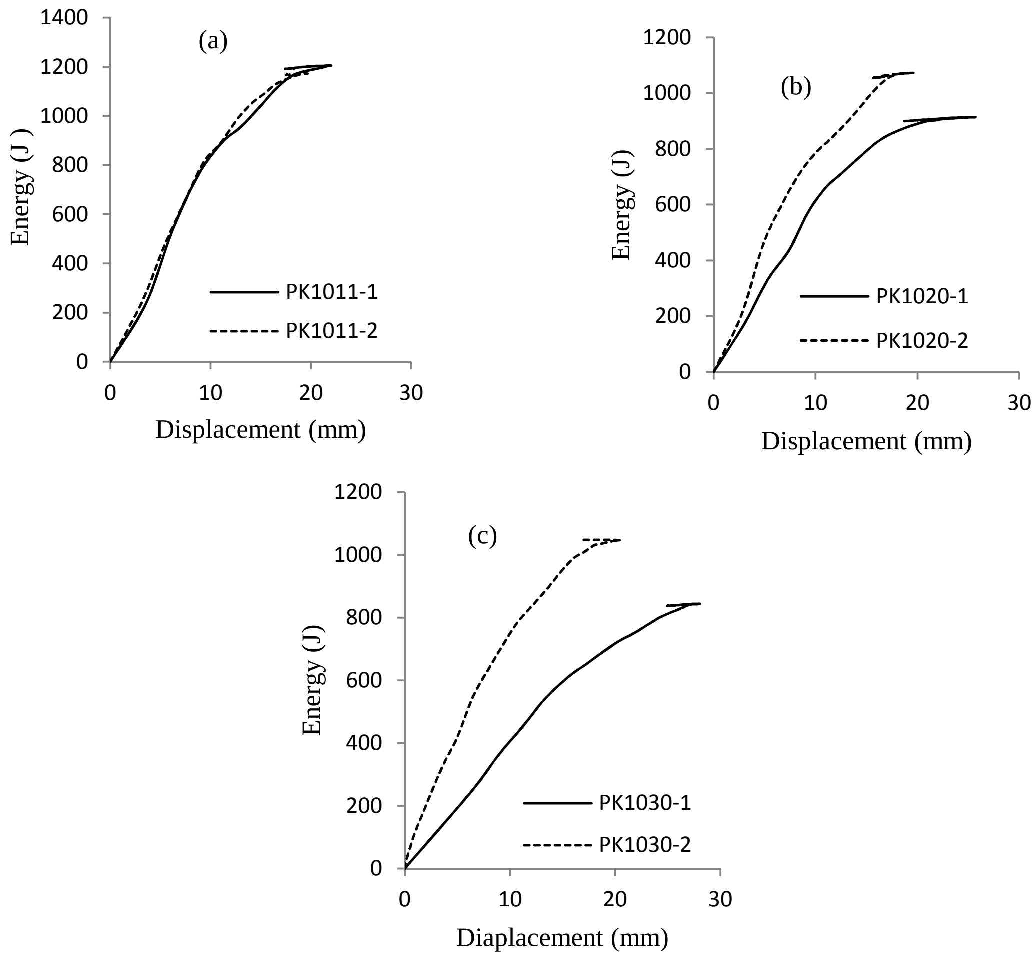

Fig. 13 Absorbed energy-mid-span displacement curves

Energy-displacement curves are obtained from impact load-time and displacement in mid-span-time curves are given in Fig. 13. Energy absorption amount of RC plates in same sizes were changed due to supporting. Amount of total energy absorbed by PK1011-1 plate is %2.7 more than PK1011-2 plate and energy absorbed by PK1020-1 is %17 less than PK1020-2 plate. In similar energy absorbed by PK1030-1 plate is %24.5 less than PK 1030-2 plate. As it can be seen Fig 13-(a), support condition has not much effect on total absorbed energy amount in PK1011 plates. However, energy absorbing is decreased by increase of span size in fixed and free supported plates. This decrease is greater in the free supported RC plates (see Fig. 13(b)-(c)).

Kennedy (1976) has classified behaviors under impact load for RC elements in two main groups. These are local damage patterns (perforation, scabbing, spalling) and global damage patterns (due to bending and shear). Local damage patterns are mostly limited to the area of contact between the impacted object and the target. In particular, the failure patterns that occurred at the bottom faces of RC plates are effective in determining the type of damage modes. Amount of absorbed energy in structural elements under impact loads in RC structures and construction

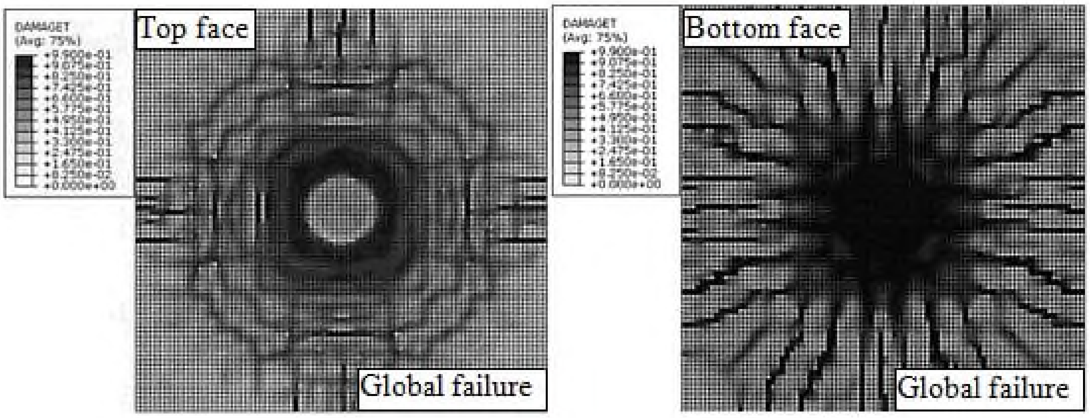

Fig. 14 Damage conditions due to changes in d_t at PK 1011-1 plate

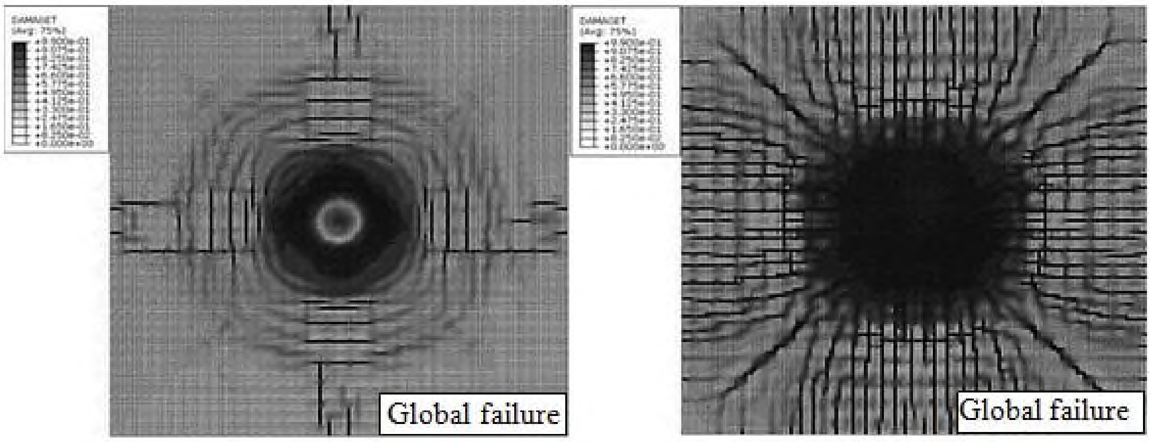

Fig. 15 Damage conditions due to changes in dt at PK 1020-1 plate

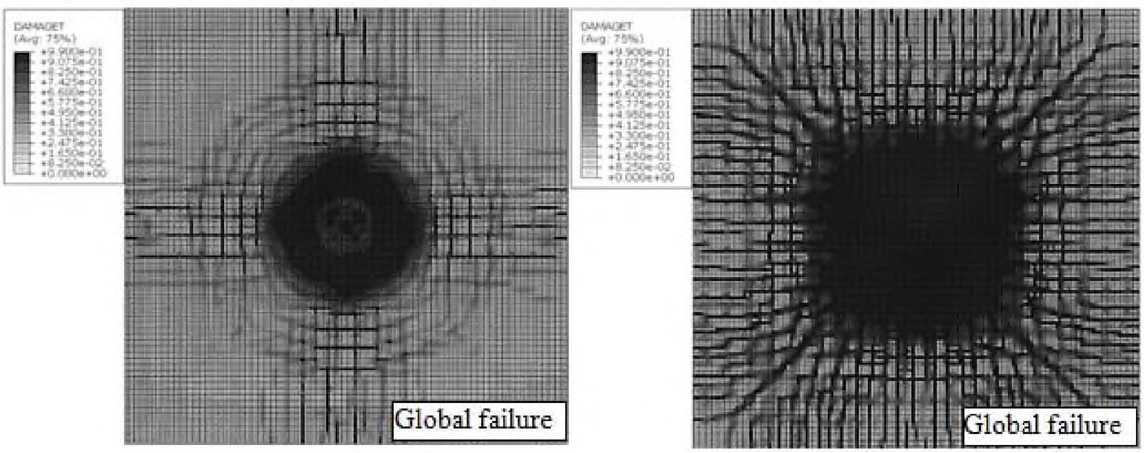

Fig. 16 Damage conditions due to changes in dt at PK 1030-1 plate

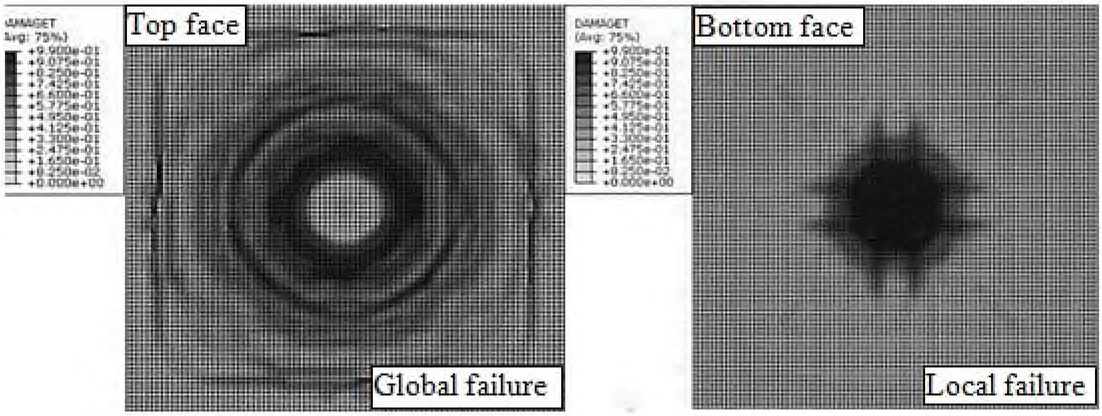

Fig. 17 Damage conditions due to changes in dt at PK 1011-2 plate

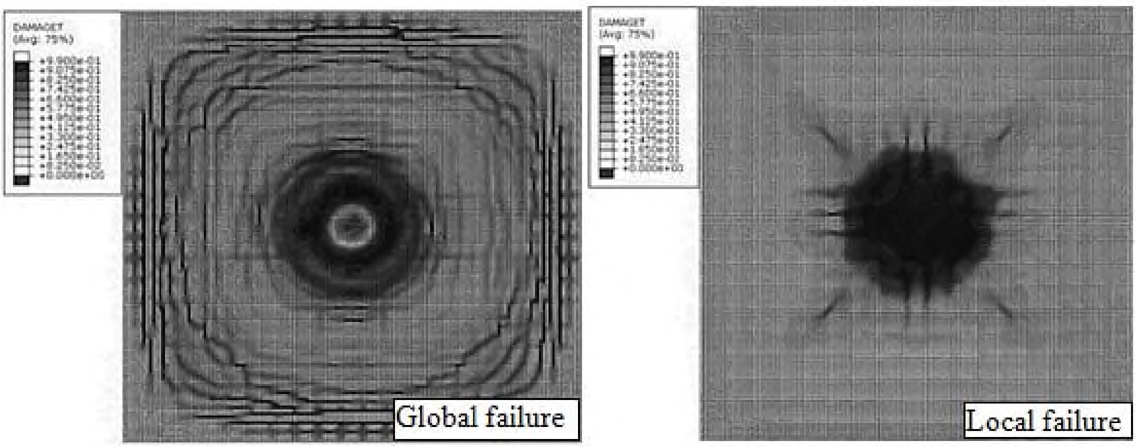

Fig. 18 Damage conditions due to changes in dt at PK 1020-2 plate

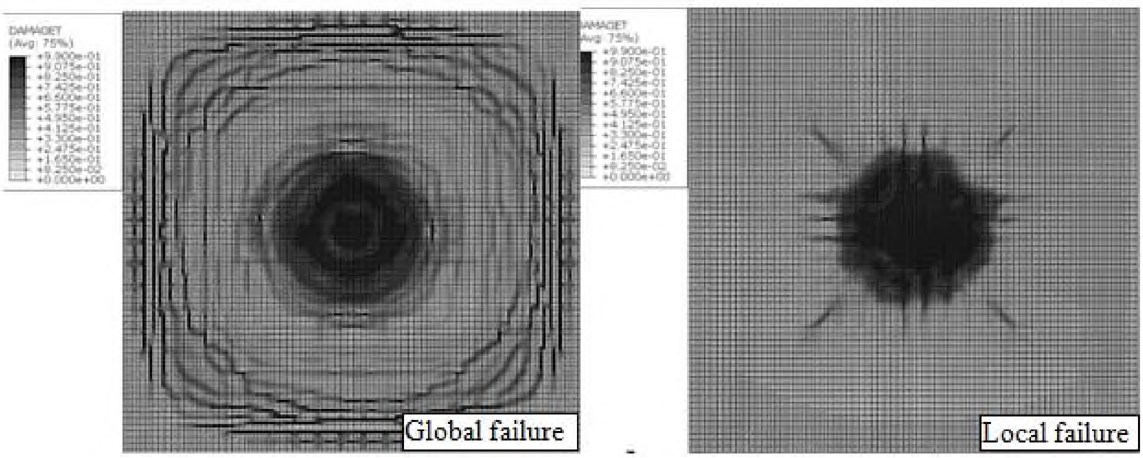

Fig. 19 Damage conditions due to changes in dt at PK 1030-2 plate

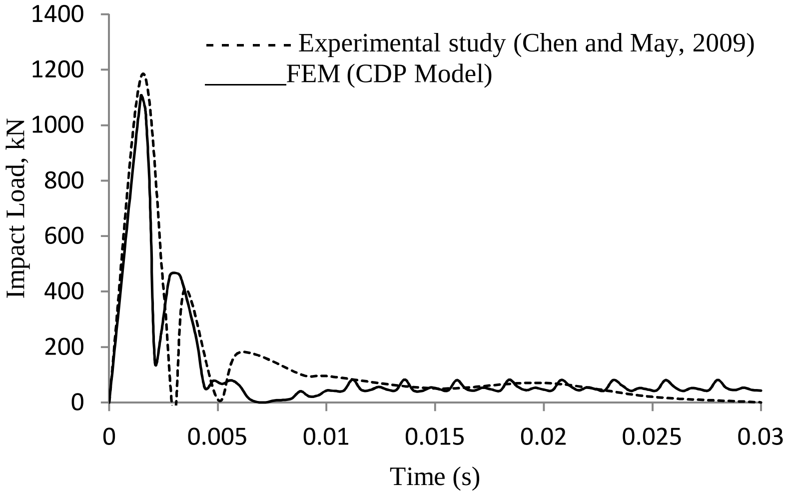

Fig. 20 Comparison between impact load-time obtained from FEM and experimental study

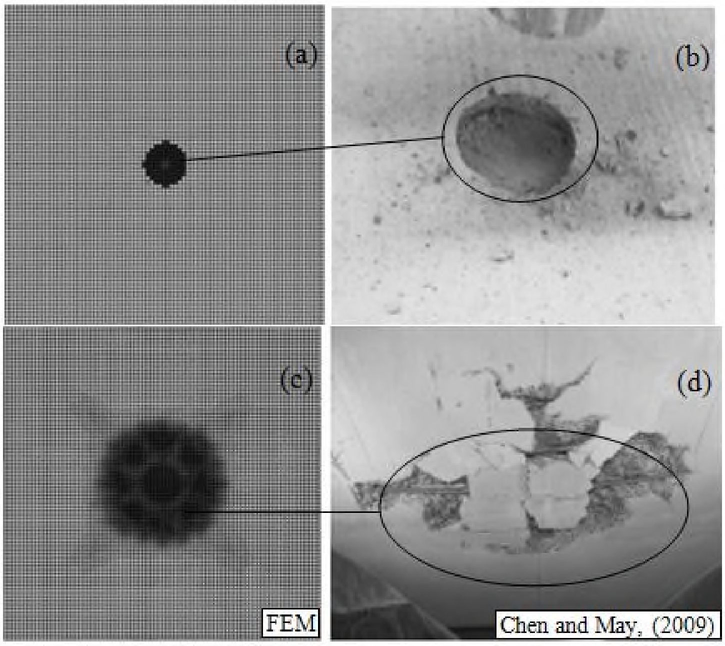

Fig. 21 Comparison between damage pattern obtained from FEM and experimental study

elements are related with such behaviors. When possible damage situations occurred by impact and evaluated with energy absorbing capacity of the plates, it is seen that in RC plates that are fitted freely to supports there is increase in tensile cracks due to bending by the increase in plate span (see Fig. 14 to 16). There are damage patterns are observed for fixed supported plate as not to be deflection but with damages concentrated on contact surface (see Fig. 17 to 19). As it can be seen from these figures and Table 3 fixed supported plates are absorbed much more energy. In this situation absorbed energy amount due to local damage patterns are higher than the global damage patterns.

Within the scope of this study comparison is made for similarity between CDP material model used for impact load effect analysis that are obtained from RC plates with the results that are obtained from previously experimental studies. For this aim, the 2330×2330×150 mm sized fixed supported RC plates that was used by Chen and May (2009) in experimental studies, is analyzed by using CDP material model. At the end of the analysis impact load-time curve and damage patterns in RC plate under impact load are compared with each other (see Figs. 20 and 21).

Maximum impact load is obtained as 1103 kN by considering CDP material model in analysis. Experimental studies that are conducted by Chen and May (2009) is obtained as 1180 kN. In experimental studies after the experiments diameter of the damaged region is given as 700 mm. In the analysis made by the CDP model is approximately 800 mm. At the end of this study, maximum impact load values obtained from numerical analysis were approximately similar to the values obtained from experimental studies.

7. Conclusion

The behavior of six RC plates under impact loading were examined numerically. The RC plates were modeled with two different support conditions and three different span sizes. The damage patterns, absorbed energies, impact load-time and displacement-time curves were compared and discussed. The conclusion drawn from the results obtained in this study are as follows

• The difference between the maximum impact load values obtained depending on the plate supporting conditions increased with the increase of plate span.

• In free supported plates, the maximum mid-span displacement values are increased by increase of plate opening. However, the span size has no considerable effect on fixed RC plates.

• Supporting condition and plate span size both effected the energy absorbing capacity significantly. Energy absorbing capacity was decreased by increase of span size in fixed and free supported plates. This decrease is greater in the free supported plates.

• It is observed that, the global damages that occurred in free support RC plates were caused by the effect of bending.

• Global damages occurred in all plates subjected to impact loads. However, the local damages only occurred at the bottom faces of the fixed support plates.

• It is observed with the guidance of numerical analyses and experimental studies in scanned literature for determining the damage patterns and maximum impact load of exposed impact load RC plates, CDP model gave proper results.

References

ABAQUS/CAE v6.12 Programme, Dassault Systemes Simulia Corp. Providence, RI, USA.

ABAQUS Analysis User's Manual (2008), Version 6.8

Abbas, H., Gupta, N.K. and Alam, M. (2004), "Nonlinear response of concrete beams and plates under impact loading", *Int. J. Impact Eng.*, **30**(8), 1039-1053.

Ammann, H. and Nussbaumer, H. (1995), *Behavior of concrete and steel under dynamic actions, Vibrations problems in structures: Practical guide*, Springer Science & Business Media, Berlin, Germany.

Chen, Y. and May, I.M. (2009), "Reinforced concrete members under drop-weight impact", *Struct. Build.*, **162**(2_3), 45-56.

Hibbitt, H., Karlsson, B. and Sorensen P. (2011), *ABAQUS Analysis user's manual version 6.11*, Dassault Systèmes Simulia Corp. Providence, RI, USA.

Kamali, A.Z. (2012), "Shear strength of reinforced concrete beams subjected to blast loading", Masters of Thesis, Royal Institute of Technology, Stockholm, Sweden.

Lee, J. and Fenves, G. (1998), "Plastic-damage model for cyclic loading of concrete structure", *Eng. Mech.*, **124**(8), 892-900.

Lubliner, J., Oliver, J., Oller, S. and Onate, E. (1989), "A plastic-damage model for concrete", *Solid. Struct.*, **25**(3), 299-326.

Malm, R. (2006), "Shear cracks in concrete structures subjected to in-plane stresses", Licentiate Thesis, Royal Institute of Technology, Stockholm, Sweden.

Malm, R. (2009), "Predicting shear type cracks initiation and growth in concrete with nonlinear finite elements methods", Ph.D. Dissertation; Royal Institute of Technology, Stockholm, Sweden.

Martin, O. (2010), "Comparison of different constitutive models for concrete in ABAQUS-explicit for missile impact analyses", JRF Scientific and Technical Report, European Commission Joint Research Centre Institute for Energy, Netherlands.

Perumal, R. (2014), "Performance and modeling of high-performance steel fiber reinforced concrete under impact loads", *Comput. Concrete*, **13**(2), 255-270.

Sawamoto, Y., Tsubota, H., Kasai, Y. and Koshika, N. (1998), "Analytical studies on local damage to reinforced concrete structures under impact loading by discrete element method", *Nucl. Eng. Des.*, **179**(2), 157-177.

Schellenberg, K., Volkwein, A., Roth A. and Vogel, T. (2007), "Large-scale impact tests on rock fall galeries", *Proceedings of the 7th International Conference on Shock & Impact Loads on Structures,* Beijing, China.

Trivedi, N. and Singh, R.K. (2013), "Prediction of impact induced failure modes in RC slabs through nonlinear transient dynamic finite element simulation", *Ann. Nucl. Energy.*, **56**, 109-121.

Zielinski, A.J. (1984), "Concrete structures under impact loading rate effects", Report 5-84-14, TH Delft, Netherlands.

Zineddin, M. and Krauthammer, T. (2007), "Dynamic response and behavior of reinforced concrete slabs under impact loading", *Int. J. Impact Eng.*, **34**(9), 1517-1534.

CC